In vitro labelling of mouse embryonic stem cells with SPIO nanoparticles

J. Krejčí[1], J. Pacherník[3], A. Hampl[2,4] and P. Dvořák[2,4]

[1] *Institute of Biophysics, Academy of Sciences of the Czech Republic, v.v.i., Královopolská 135, 612 65 Brno, Czech Republic*
[2] *Institute of Experimental Medicine, Academy of Sciences of the Czech Republic, v.v.i., Vídeňská 1083, 140 00 Prague 4, Czech Republic*
[3] *Faculty of Science, Masaryk University, Kotlářská 2, 602 00 Brno, Czech Republic*
[4] *Faculty of Medicine, Masaryk University, Kamenice 5, 625 00 Brno, Czech Republic*

Abstract. Labelling of mammalian cells with superparamagnetic iron oxide (SPIO) nanoparticles enables to monitor their fate *in vivo* using magnetic resonance imaging (MRI). However, the question remains whether or not SPIO nanoparticles affect the phenotype of labelled cells. In the present study, the effects of SPIO nanoparticles from two producers on the growth and differentiation of mouse embryonic stem (ES) cells *in vitro* were investigated. Our observations have shown that SPIO nanoparticles have no effect on the self-renewal of ES cells. Subsequently, we studied the effect of SPIO on the formation of embryoid bodies and neural differentiation of ES cell in monolayer culture. The cavitation of embryoid bodies was partially inhibited and neural differentiation was supported regardless the type of SPIO nanoparticles used. Thus for the first time we documented the effects of SPIO nanoparticles on ES cells and their differentiation.

Key words: Embryonic stem cells — Differentiation — Magnetic labelling — SPIO nanoparticles

Introduction

Embryonic stem (ES) cells are derived from the inner cell mass of the pre-implantation blastocyst and can both self-renew and differentiate into all cell types of the adult body. This capability provides the basis for considering the human ES cells as a novel and unlimited source of cells for applications in the therapy of serious diseases and (traumatogenic) damages caused by injury. However, for practical application of the cell therapy it is essential to find appropriate and efficient methods for monitoring the fate of cells, their migration and final position in the patient's body. Contrast agents containing superparamagnetic iron oxide (SPIO) nanoparticles detectable by magnetic resonance imaging (MRI) are used in human medicine for investigations of the gastrointestinal tract (Hahn et al. 1990), liver and spleen (Hamm et al. 1994; Reimer and Tombach 1998) or lymph nodes (Anzai et al. 1994) pathologies. The method exploiting contrast agents with iron nanoparticles was used by Sipe et al. (1999) for intracellular labelling of human mononuclear cells (lymphocytes and monocytes). Cells labelled using this method are detectable by MRI *in vivo* and therefore labelling with SPIO nanoparticles may also be feasible for ES cells.

The definitive fate of SPIO nanoparticles in the body is given by its general metabolism. Due to dextran-based coating the nanoparticles are degradable. The iron enters the plasma iron pool and is subsequently incorporated into red cell production and other natural uses of iron. Eventually, it is secreted from the body as the body iron store. The amount of iron oxide that would be required for clinical MRI is small in comparison with the physiological iron stores (Reimer et al. 1995). Thus compared with other MRI agents, the toxicity of the SPIO agents is low and they may be easily used in medical and veterinary diagnostic (Simonsen et al. 1999).

Recently, there have been several reports using various SPIO nanoparticles to label mammalian cells and to monitor their positions or migration *in vivo* by MRI after transplantation into the animal model (Jendelová et al. 2003; Arbab et al. 2005; Hauger et al. 2006; He et al. 2007). Nanoparticles

Correspondence to: Jana Krejčí, Institute of Biophysics, Academy of Sciences of the Czech Republic, v.v.i., Královopolská 135, 612 65 Brno, Czech Republic
E-mail: krejci@ibp.cz

may probably enter cells by various mechanisms with the receptor-independent endocytosis being the one that has been demonstrated to function in wide spectrum of cell types including ES cells (Bulte et al. 2001; Jendelová et al. 2004). The actual presence of nanoparticles in cytoplasm of mouse ES (mES) cells has been clearly shown by transmission electron microscopy (TEM) (Jendelová et al. 2004).

In some reports, the SPIO nanoparticle-labelled ES cells were also used (Jendelová et al. 2004; Tallheden et al. 2006). However, our knowledge about the effects of SPIO on the qualities of ES cells is still limited. We know that ES cells labelled with SPIO migrate in the tissue of the organism, differentiate and adopt new features dependent on their position in the target tissue (Björklund et al. 2002; Jendelová et al. 2004). However, the efficiency of magnetic labelling of ES cells, the effects on cell behaviour, division and/or differentiation processes have not been conclusively determined. It is important to note that after cell transplantation, the new environment influences the therapeutic effects due to the adaptability of ES cells and magnetic labelling can play a role during this process. Therefore in our pilot study we tested the effects of two commercially accessible SPIO nanoparticles, i.e. Endorem (Guerbet, France) and Resovist (Schoeller, Germany), on growth and differentiation of mES cells *in vitro*. At the present time, both of these agents have been approved for use as contrast solutions for diagnostics of liver or spleen diseases.

Materials and Methods

Culture and differentiation of ES cells

Undifferentiated mES cells, D3 line (mES D3; Doetschman et al. 1985) were routinely grown on mytomycin C-treated STO fibroblasts in Dulbecco´s modified Eagle´s medium (Gibco) supplemented with 20% fetal calf serum (PAA Laboratories GmbH), 100×10^{-3} mol/l non-essential amino acids (Gibco), 0.05×10^{-3} mol/l β-mercaptoethanol (Sigma), 100 U/ml penicillin, 0.1 mg/ml streptomycin (Gibco), and 1000 U/ml recombinant leukemia inhibitory factor (LIF; Chemicon International). Before experiments, the mES D3 cells were adapted to feeder-free culture according to Smith and Hooper (1987), here mentioned as standard condition. Passaging was executed every 3 days; subculture ratio was 1 : 10. The proliferation activity of ES cells in culture with and without SPIO was tested by WST-1 assay (Roche) according to manufacturer's instructions in every passage.

The differentiation of ES cells to embryoid bodies (EBs) was performed by hanging drop technique in complete ES media without LIF (Robertson 1987; Keller 1995). After 4 days growing, EBs were transferred into bacteriological dishes and fresh media and dishes were replaced every 2 days.

Neural differentiation in monolayer was induced by seeding mES D3 cells into culture medium without LIF. After 2 days, the cells were washed with PBS and the serum containing medium was replaced by serum-free DMEM/F12 (Gibco) supplemented with insulin, transferrin, selenium (ITS; Gibco), 2 μg/ml fibronectin (Sigma), 0.1×10^{-6} mol/l retinoic acid (Sigma) and 500 U/ml LIF for further 2 days and subsequently in DMEM/F12 medium with ITSF supplement alone. Medium was changed every 2 days (Pacherník et al. 2002, 2005).

Labelling cells by SPIO nanoparticles

Both SPIO particles tested have standard size. Endorem SPIO nanoparticles (Guerbet, France) are 80–150 nm in diameter and the iron oxide crystal is 4.8–5.6 nm in size coated with dextran. Resovist SPIO nanoparticles (Schering, Germany) contain carbodextran-coated crystal 4.2 nm in size and hydrodynamic diameter is 62 nm (Sipe et al. 1999; Wang et al. 2001; Vogl et al. 2003). To test the effect of SPIO particles on growth of undifferentiated mES D3 cells we used dose 112.4 mg iron per milliliter of culture medium. Cells were passaged every three days; the subculture ratio was 1 : 10. Fresh SPIO nanoparticles were added to the culture media after each passage during the test. For differentiation experiments, the mES D3 cells were pre-labelled with SPIO nanoparticles within two passages before induction of differentiation. After induction of differentiation, the dose of iron was decreased to 28.1 mg per ml for both Endorem and Resovist.

Immuno- and cytochemistry

The undifferentiated cells were immunocytochemically stained for the stage specific embryonal antigen 1 (SSEA-1) using TEC-01, mouse monoclonal antibody (provided by Dr. P. Dráber, Institute of Molecular Genetic, Prague, Czech Republic). Differentiated cells were stained for glial fibrillary acidic protein (GFAP) using goat polyclonal antibody against GFAP (sc-6170; Santa Cruz Biotechnology) as described previously (Pacherník et al. 2002; Kroupová et al. 2006).

Prussian blue staining of ferric iron was performed as follows: cells were fixed with 4% paraformaldehyde, washed with PBS, incubated for 30 min with 2% potassium ferrocyanide (Perl´s reagent) in 6% hydrochloric acid, washed with PBS and counterstained with Nuclear fast red (Frank et al. 2003).

Western blot analysis

For western blot analysis, cell samples were prepared as follows: ES cells and/or EBs were washed twice with PBS

(pH 7.2) and lysed in sodium dodecyl sulphate (SDS) lysis buffer (50×10^{-3} mol/l Tris-HCl, pH 7.5; 1% SDS; 10% glycerol). Protein concentrations were determined using DC Protein assay kit (Bio-Rad). Lysates were supplemented with bromphenol blue (0.01%) and β-mercaptoethanol (1%), and incubated for 5 min at 95°C. Equal amounts of total protein (10 μg) were subjected into 10% SDS-PAGE. After being electrotransferred onto polyvinylidene difluoride membrane (Immobilon-P, Sigma), proteins were immunodetected using appropriate primary and secondary antibodies, and visualized by ECL+Plus reagent (Amersham Pharmacia Biotech) according to manufacturer's instructions. The antibodies used were as fallows: rabbit polyclonal antibody against Oct 3/4 (sc-9081), goat polyclonal antibodies against GAP-43 (sc-7457), GFAP (sc-6170), Lamin B (sc-6217) – all from Santa Cruz Biotechnology, and mouse monoclonal antibody against neuron-specific class β III tubulin isotype (TU-20) – provided by Dr. P. Dráber (Institute of Molecular Genetic, Prague, Czech Republic). After immunodetection, each membrane was stained by amidoblack to confirm equal protein loading.

Semiquantitative reverse transcription and PCR

Total RNA was extracted from cell using RNeasy Mini Kit (Qiagen). cDNA was synthesized according to the manufacturer's instructions for M-MLV reverse transcriptase (Gibco BRL). Primers and PCR conditions were as follows (primer sequence; annealing temperature/number of cycles/product size): GATA-4 (5`-GAAAACGGAAGCCCAAGAACC-3`, 5`-TGCTGTGCCCATAGTGAGATGAC-3`; 54°C/32/186 bp); Brachyury (5`-GAGAGAGAGCGAGCCTCCAAAC-3`, 5`-GCTGTGACTGCCTACCAGAATG-3`; 56°C/29/230 bp); HPRT (5`-CTTGCTGGTGAAAAGGACCTCTC-3`, 5`-CAAATCAAAAGTCTGGGGACGC-3`; 56°C/24/350 bp) (Ešner et al. 2002). Before being used for cDNA quantification, the range of linearity was determined for each primer set. The PCR products were separated on 1.5% agarose gels and visualized by ethidium bromide staining.

Statistical analysis

Data are expressed as mean ± SEM. Statistical analysis was assessed by one-way ANOVA. $p < 0.05$ were considered to be statistically significant.

Results

In the present study, the model ES cells were magnetically labelled by adding two types of agents containing SPIO nanoparticles that are detectable by MRI *in vivo*. The consequently labelled and control mES D3 cells were cultured for 10 passages under undifferentiated conditions and for 20 days after induction of differentiation (EBs formation and neural differentiation in monolayer). Differences in properties of ES cells during these processes caused by the presence of SPIO nanoparticles in ES cells were determined.

Labelling of ES cells with SPIO nanoparticles

Abundant uptake of ferumoxides (SPIO) in the ES cells was revealed by Prussian blue staining. No stainable iron was detected in the control ES cells (cells unlabelled with SPIO, data not shown). We observed a high efficiency of SPIO labelling in both types of nanoparticles. After two passages with SPIO nanoparticles we detected the presence of iron in 80–85 % of ES cells (Fig. 1A). Compared to Endorem the labelling efficiency of Resovist nanoparticles appeared to be slightly higher. It was probably due to their higher adhesiveness to the cell surface (Fig. 1B).

SPIO nanoparticles do not affect the self-renewal of ES cells

The proliferation of SPIO labelled cells was measured using WST-1 reagents, and was compared with proliferation of control cells. We detected no differences at the analysed time intervals (Fig. 2A) between control and SPIO-labelled cells.

In the same experiment, the undifferentiated status of mES D3 cells was also analysed. Both the SPIO-labelled and control ES cells expressed markers that are characteristic for undifferentiated ES cells. Fig. 1C shows the presence of membrane SSEA-1 in control and SPIO labelled ES cells detected by immunocytochemistry. The detection of the transcription factor Oct 3/4 protein level by the western blot method is shown in Fig. 2B. As presented, we did not observe any difference in the expression of SSEA-1 and Oct 3/4 between control and SPIO (Endoderm or Resovist) labelled ES cells. In parallel, no apoptosis was detected after SPIO labelling compared to control cells, neither by western blot detection of the Lamin B cleavage product (Fig. 2B) nor by microscopic observation of changes in ES colonies or cell morphology and appearance of apoptotic bodies (data not shown). Thus labelling with SPIO has no effect on the proliferation of ES cells and their self-renewal.

Effects of SPIO on differentiation of ES cells into EBs

mES D3 cells were pre-labelled with SPIO during two passages before the induction of differentiation. First we tested how magnetic labelling affected the formation of 3D-structures known as EBs. At the early phase of differentiation, the EBs were compact and morphology of the control and

A

Number of passage	Labelled cells (%)	
	Endorem	Resovist
1	40.8 ± 5.9	
2	84.3 ± 7.0	> 85
3	80.9 ± 6.1	

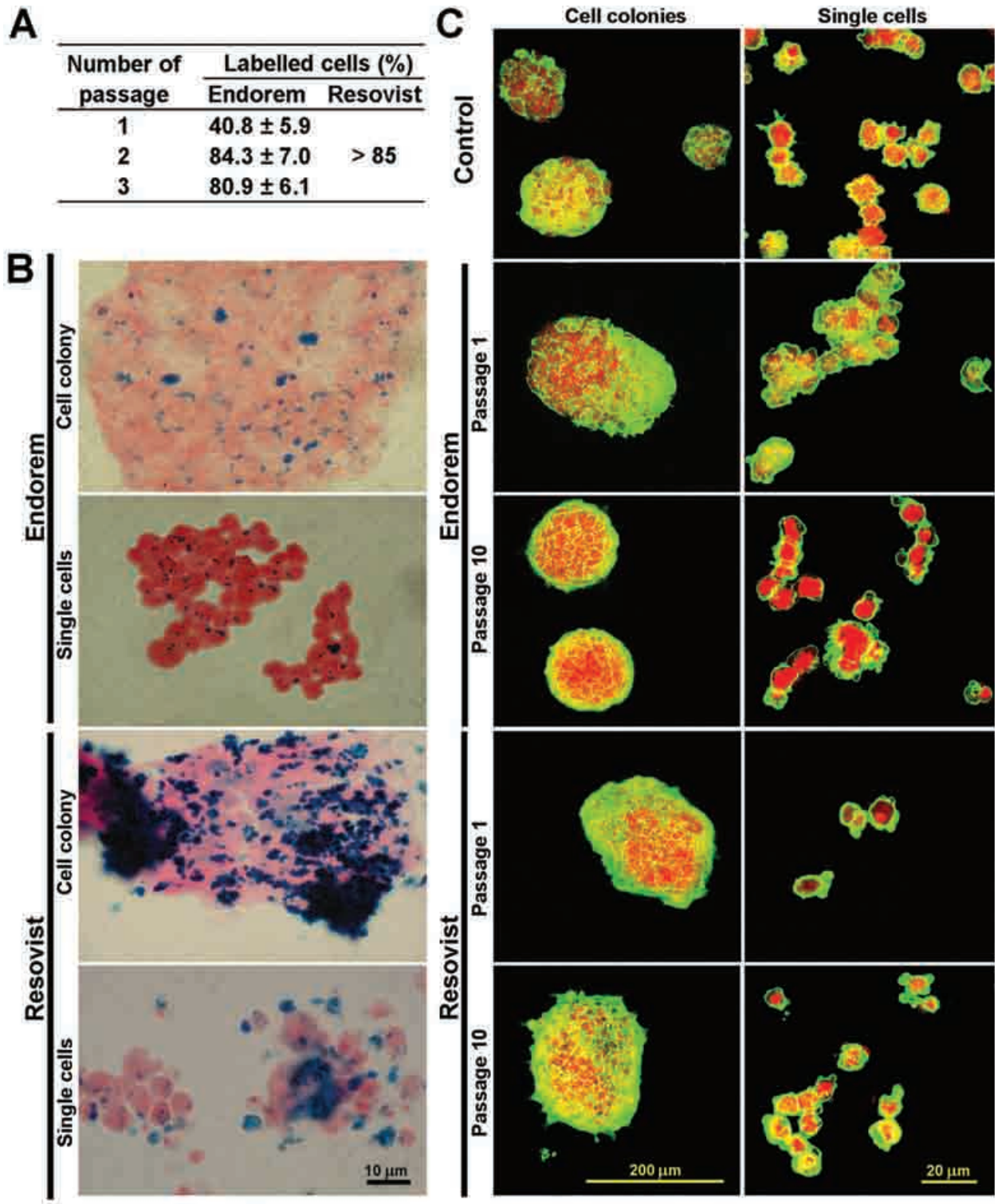

Figure 1. Study of undifferentiated mES D3 cells growing in presence of SPIO nanoparticles. **A.** Percentage of magnetic labelled cells after cultivation of ES cells in presence of SPIO nanoparticles for 1, 2 and 3 passages. In passages 4–10, the percentage of iron positive cells was similar with passage 3. **B.** Detection of SPIO nanoparticles by Prussian blue and Nuclear fast red staining in ES cells grown in cell colonies and in single cells after trypsinization. **C.** Detection of embryoglycan epitope TEC-01 (homolog of SSEA-1; green) in control and SPIO labelled undifferentiated ES cells grown in cell colonies and in single cells after trypsinization. Cell nuclei were stained with propidium iodide (red). Figure shows immunocytochemistry detection in passage 1 and 10.

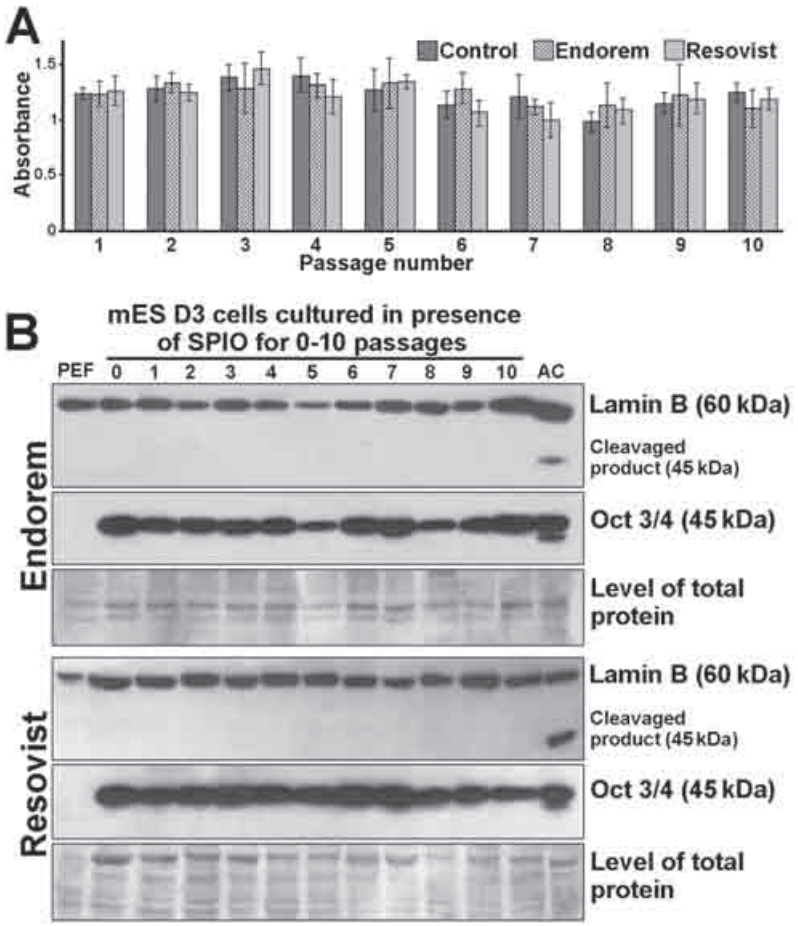

Figure 2. A. Comparison of proliferation of control and SPIO labelled mES D3 cells during 10 passages under standard conditions. In every passage, the ES cells were subcultivated 1 : 10. After growth for 3 days, the WST-1 kit was used for detection of the cell number in all three experimental groups. **B.** The detection of Lamin B cleavage and protein level of Oct 3/4 by western blot. ES cell were cultivated for 10 passages in presence of SPIO nanoparticles. Overgrowth ES cells were used as apoptic control (AC), which is characterized by presence of cleavage Lamin B. Primary mouse embryonic fibroblasts (PEF) were used as a negative control for Oct 3/4 detection.

SPIO-labelled EBs did not differ (Fig. 3A). However, on day 10 of differentiation (day of differentiation – D.d.), the majority of control EBs cavitated, while cavitation of EBs formed from SPIO pre-labelled cells was delayed. As is shown in Fig. 3D, cavity was observed in 87.5% of control EBs, while only 49.4% of Endorem and 51.7% of Resovist labelled EBs, respectively, cavitated. The absence of cavity in EBs from SPIO pre-labelled ES cells was associated also with a lower volume of EBs as compared with control EBs (Fig. 3B). The RT-PCR analyses of endoderm-specific GATA-4 mRNA and marker of early mesoderm Brachyury documented the observed differences in EBs growth. Both transcripts were undetectable in undifferentiated ES cells (Fig. 3C). In control EBs, the GATA-4 transcript level continuously increased as cells in EBs differentiated. In EBs from SPIO pre-labelled ES cells, the GATA-4 transcript also appeared during differentiation of EBs, but in our tested time intervals the level of GATA-4 was decreased on day 10 of EBs differentiation (Fig. 3C). Thus the expression of GATA-4 seems to take a biphasic regulation in SPIO pre-labelled EBs but not in control EBs. The expression of the Brachyury transcript was high on D.d. 5, only slight on D.d. 10 and undetectable on D.d. 15 and 20 in control EBs (Fig. 3C). In the case of SPIO pre-labelled EBs, the level of the Brachyury transcript was not as high as in control EBs on day 5. Moreover the dynamics of Brachyury expression between the controls (unlabelled) and SPIO pre-labelled EBs also differed, and also among the SPIO pre-labelled EBs. In Endorem pre-labelled EBs the level of the Brachyury transcript was still high on day 10, while in the Resovist pre-labelled EBs the overall expression of the Brachyury transcript was lower but it was discontinuous and detectable also in 15-day-old EBs (Fig. 3C). We assume that variation in the expression of GATA-4 and Brachyury transcripts

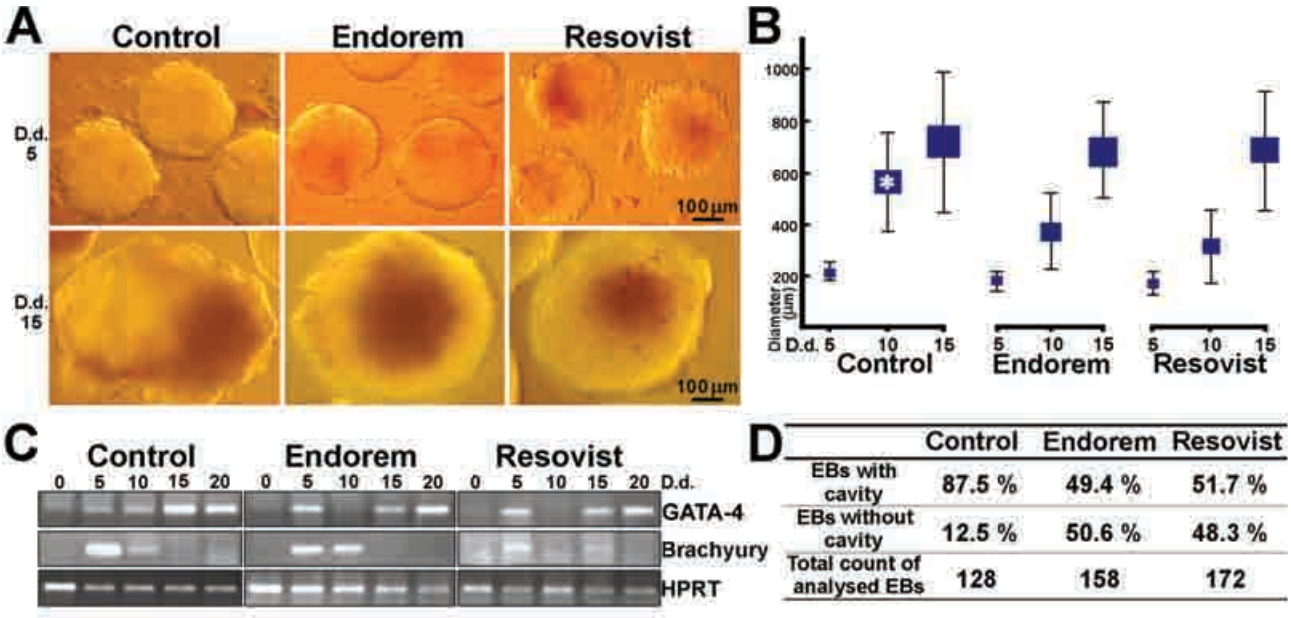

Figure 3. Differentiation of SPIO pre-labelled mES D3 cells to the three-dimensional embryoid bodies (EBs). **A.** Morphology of control EBs and EBs formed from SPIO pre-labelled cells at day of differentiation (D.d.) 5 and 15. **B.** Size of tested EBs in D.d. 5, 10 and 15. Star marks statistical significant difference ($p < 0.05$) in size of control EBs in comparison with size of EBs increased from SPIO pre-labelled cells at D.d. 10. **C.** RT-PCR analysis of endoderm (GATA-4) and mesoderm (Brachyury) specific genes in EBs differentiated for 20 days. The hypoxantyne-guanine phosphoribosyltransferase (HPRT) gene was used as control for cDNA integrity. **D.** Percentage of control and SPIO pre-labelled EBs with and without cavity after 10 D.d.

corresponds with the retardation of SPIO pre-labelled EBs differentiation as described above.

Effects of SPIO on differentiation of ES cells into neural cells in monolayer culture

Second, we studied the effects of SPIO labelling on more specific differentiation such as the induction of ES cells into neural differentiation by LIF depletion in monolayer culture. The cells rounded up and started to create protrusions. Although after start of cell culture in serum-free conditions (DMEM/F12 with ITS, retinoid acid, fibronectin and LIF) a majority of such cells died, the remaining cells gave rise to a three-dimensional structure that later developed into adhered growing spheroid-colonies with expanding neuron-like cells. Thus differentiated ES in all tested groups of cells adopted neural morphology from day 10 after withdrawal of growth factor (LIF) responsible for the undifferentiated state (Fig. 4A). In agreement with their neural morphology, we also detected the presence of neural specific proteins such as GFAP, GAP-43 and neuron-specific β III tubulin (Fig. 4B). Both GAP-43 and β III tubulin were well detected on D.d. 10 and 15. Later, on D.d. 20, the protein level of these markers decreased, probably through overgrowth of the terminally differentiated neural cells by other, here non-specified cell populations. It seems that when the ES cells were pre-labelled with SPIO, slightly higher pro-neural differentiation potentials were detected. The neuron specific β III tubulin was more expressed in SPIO pre-labelled cells than in control cells. The level of neuron-specific β III tubulin was the highest on day 15 in Endorem pre-labelled cells and the earliest detection was seen in Resovist pre-labelled cells on day 8 of neural differentiation. All comparisons were achieved with control cells differentiated by the same protocol (Fig. 4B). The level of the other pro-neural protein marker GAP-43 was the highest in control cells on D.d. 10 and was lower in SPIO pre-labelled cells. In all three experimental groups, the appearance of GAP-43 correlated with the expression of neuron-specific β III tubulin (Fig. 4B). The astrocyte-specific GFAP protein was detected with the western blot only in Endorem pre-labelled cells on D.d. 20 (Fig. 4B). The more abundant astrocyte population in control and labelled cells was also documented by immunocytochemistry detection of GFAP positive cells (Fig. 4C). The GFAP positive cells were well distinguishable among the SPIO labelled cells on D.d. 8, but no GFAP positive cells were detected in the control cell population in this time interval. The GFAP positive cells were detected also in control cells until D.d. 10. At the time when these cells were detected, they represented less than 5% of the total number of differentiated cells in all experiments.

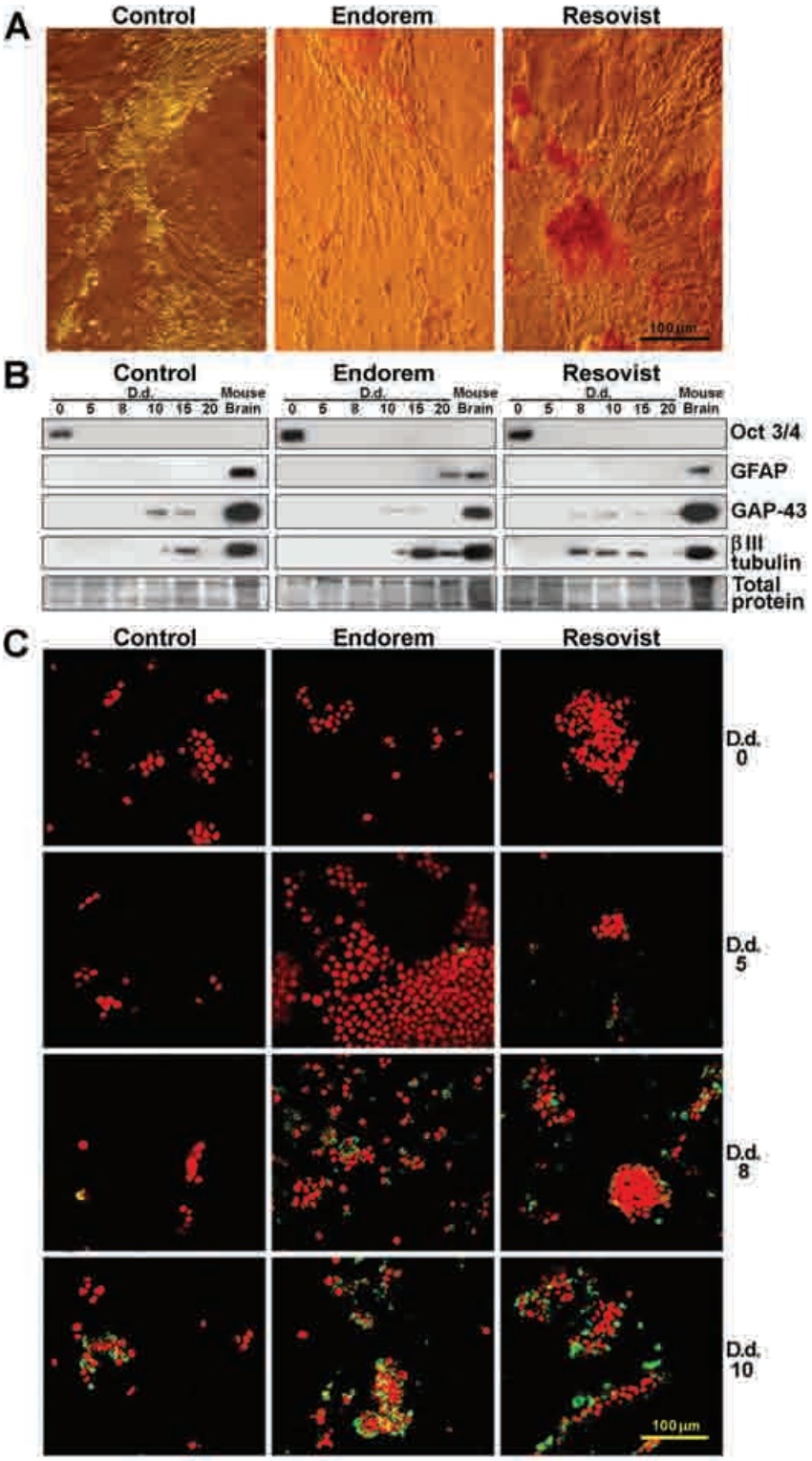

Figure 4. Neural differentiation of mES D3 cells induced in monolayer culture. **A.** Morphology of ES cells induced to neural differentiation after 15 days of differentiation (D.d.). **B.** Western blot analysis of transcription factor Oct 3/4 specific for undifferentiated state of ES cells and neural specific protein markers (GFAP, GAP-43, β III tubulin) in differentiating ES cells. **C.** Immunocytochemistry detection of GFAP-positive cells (green) in control and SPIO labelled ES cells at 0, 5, 8 and 10 D.d. Cell nuclei were stained with propidium iodide (red).

Discussion

The objective of the present study was to determine the effects of SPIO nanoparticle labelling on *in vitro* cultured and differentiating model ES cells and to verify if their application is suitable in developing cell transplantation therapies.

The labelling of various cells selected for transplantation therapies and their visualization in target tissue and organs with MRI provides a non-invasive method for the study of their further fate *in vivo* (Bulte et al. 1999, 2002; Sipe et al. 1999; Frank et al. 2003; Jendelová et al. 2003, 2004; He et al. 2007; Syková and Jendelová 2007). The effects of different types of SPIO and/or their modifications on features of labelled cells may be expected. Previously, we have demonstrated by TEM the ability of mouse ES cells to accumulate nanoparticles in their cytoplasm (Jendelová et al. 2004). In our pioneered study we have tested and compared the effects of Endorem and Resovist (two different agents containing SPIO nanoparticles) on growth and neural differentiation of mES D3 cells *in vitro*. Both of the tested magnetic substances may be used for ES cell labelling without further modifications as our present and previously published results proved (Jendelová et al. 2004).

A 112.4 mg/ml concentration of iron was used; an approximately four times higher amount of iron than Sipe et al. (1999) used for labelling mononuclear cells. Mononuclear cells grow in a suspension of single cells and need only a few hours for sufficient SPIO labelling, while ES cells grow in cell colonies. That is why we chose (based on our preliminary test, not shown) the above mentioned higher volume of iron. As shown in our study, the efficiency of magnetic labelling by simple addition of SPIO nanoparticles to the culture medium was high in both cases of SPIO agents. This type of labelling is non-specific, not dependent on targeted membrane receptor binding (Bulte et al. 2001). A small difference was observed in the adherence of SPIO nanoparticles to the ES cell surface. It is probably the effect of distinct coating of the iron oxide crystal: Endorem – dextran and Resovist – carbodextran (Wang et al. 2001). On rat bone marrow stromal cells Horák et al. (2007) demonstrated a high significance of iron oxide coating to endocytosis of nanoparticles.

Moreover, we studied the effects on growth and properties of undifferentiated mES D3 cells. No effects of SPIO nanoparticles were proved. Although we cultured the ES cells in the presence of SPIO up to 10 passages neither Endorem nor Resovist changed the growth parameters of mES D3 cells (Fig. 2A). Neither did the detections of protein markers SSEA-1 and Oct 3/4, which mark the undifferentiated status of ES cells (Pera et al. 2000) show any changes (Figs. 1C and 2B). Thus SPIO nanoparticles have a minor or zero effect on self-renewal of ES cells. In our analyses no effect was detected. Similarly Arbab et al. (2003) earlier observed a high bio-compatibility of SPIO with the human mesenchymal stem and HeLa cells. It seems that the undifferentiated state of ES cells cultured under standard conditions is not affected by labelling with SPIO nanoparticles.

Nevertheless, for stem cell applications in transplantation therapies their differentiation derivatives are generally required. Undifferentiated cells are incompetent due to the risk of tumour formation. Accordingly, we further tested the effects of SPIO on differentiation processes of mES D3 cells using two differentiation protocols. First, the ES cells were induced to a general differentiation process using the formation of floating compact colonies calling EBs. Here, we employed the hanging drop technique followed by cultivation of growth EBs on bacteriological dishes. *In vitro* generated EBs contain cells of all three germ layers and recapitulate the early stages of embryonic development with some aspects (Martin et al. 1977; Desbaillets et al. 2000). Our experiments proved that if the ES cells had been pre-labelled with SPIO, the development of EBs was partially retarded. It was a failure in the cavitation of EBs. EBs increased from control ES cells were slightly larger than EBs from SPIO pre-labelled ES cells and cavity was present in about 90% of them. In EBs from SPIO pre-labelled ES cells, both Endorem and Resovist, we detected cavitation on day 15 of EBs differentiation approximately only in 50% (Fig. 3A,B and D). These defects in EBs development were correlated with the incorrect expression of early differentiation markers GATA-4 and Brachyury analysed here (Fig. 3C). As we and other authors observed previously, this correlation may be expected when EBs or the embryos develop incorrectly. Variations in the expression of GATA-4 and Brachyury thus marked very well the errors in both EBs and early embryo differentiation and development (Deng et al. 1994; Ešner et al. 2002).

Similarly, if the SPIO pre-labelled cells were differentiated in a monolayer culture toward neural lineages, the differences in the level and timing of neural protein markers expression were also observed as compared with the control cell population (Fig. 4B). Our results show a slightly higher pro-neural potential of SPIO pre-labelled ES cells, probably due to a stronger growth inhibitory effect of SPIO under this differentiation condition that enables differentiation to neural lineages. Deviations in differentiation affected by magnetic labelling were also observed by Kostura et al. (2004), human bone marrow-derived mesenchymal stem cells (MSCs) were labelled with Feridex (poly-L-lysine-coated nanoparticles). In accordance with our analyses, the magnetic labelled MSCs exhibited an unaltered viability and proliferation potential and they underwent normal adipogenic and osteogenic differentiation. However, in these cells there was a significant inhibition of chondrogenesis.

In summary, the results of our experiments showed that magnetic labelling of mES cells under standard conditions has undetectable effects on their self-renewal.

Typical properties of mES cells, such as the high level of the transcription factor Oct 3/4 or presence of the membrane antigen SSEA-1, were stable during cultivation for 10 passages in undifferentiated conditions in the presence of two types of tested standard size SPIO nanoparticles. Also, no apoptosis ES cells were detected. However, when the ES cells were committed to differentiation, the presence of SPIO nanoparticles in cells modified these processes. It is probably a response to double stresses, both differentiation and presence of SPIO itself. Although we did not test a broad range of different types of SPIO in the present study, a slight variation between Endorem and Resovist SPIO was observed. We therefore assume that various modifications of SPIO nanoparticles may improve their bio-compatibility and/or their improved properties may also be used for tight regulation of cell growth and differentiation to various lineages. It seems that not only the presence of magnetic particles in cells can influence their properties but that we must also consider the type of iron oxide crystal coating. Finally, it is worth noting that modulatory effect of SPIO nanoparticles may possibly occur only when undifferentiated ES cells are labelled and then induced to differentiate. Although it was not investigated in enough detail, progenitor cells can be less sensitive and thus more suited for nanoparticle labelling. In support of this view, oligodendrocyte precursors (Bulte et al. 1999) as well as mES cells-derived neural precursors (Jendelová et al. 2004) were previously successfully labelled with SPIO nanoparticles and found capable of proliferation and incorporation into living tissue.

Acknowledgements. This work was supported by the grant No. 301/08/0717 of the Grant Agency of the Czech Republic and by Ministry of Education, Youth, and Sports of the Czech Republic, grant No. 1M0021620803.

References

Anzai Y., Blackwell K. E., Hirschowitz S. L., Rogers J. W., Sato Y., Yuh W. T., Runge V. M., Morris M. R., McLachlan S. J., Lufkin R. B. (1994): Initial clinical experience with dextran-coated superparamagnetic iron oxide for detection of lymph node metastases in patients with head and neck cancer. Radiology **192,** 709–715

Arbab A. S., Bashaw L. A., Miller B. R., Jordan E. K., Lewis B. K., Kalish H., Frank J. A. (2003): Characterization of biophysical and metabolic properties of cells labeled with superparamagnetic iron oxide nanoparticles and transfection agent for cellular MR imaging. Radiology **229,** 838–846

Arbab A. S., Yocum G. T., Rad A. M., Khakoo Y., Fellowes V., Read E. J., Frank J. A. (2005): Labeling of cells with ferumoxides-protamine sulfate complexes does not inhibit function or differentiation capacity of hematopoietic or mesenchymal stem cells. NMR Biomed. **18,** 553–559

Björklund L. M., Sánchez-Pernaute R., Chung S., Andersson T., Chen I. Y., McNaught K. S., Brownell A. L., Jenkins B. G., Wahlestedt C., Kim K. S., Isacson O. (2002): Embryonic stem cells develop into functional dopaminergic neurons after transplantation in a Parkinson rat model. Proc. Natl. Acad. Sci. U.S.A. **99,** 2344–2349

Bulte J. W., Zhang S. C., van Gelderen P., Herynek V., Jordan E. K., Duncan I. D., Frank J. A. (1999): Neurotransplantation of magnetically labeled oligodendrocyte progenitors: magnetic resonance tracking of cell migration and myelination. Proc. Natl. Acad. Sci. U.S.A. **96,** 15256–15261

Bulte J. W., Douglas T., Witwer B., Zhang S. C., Strable E., Lewis B. K., Zywicke H., Miller B., van Gelderen P., Moskowitz B. M., Duncan I. D., Frank J. A. (2001): Magnetodendrimers allow endosomal magnetic labeling and *in vivo* tracking of stem cells. Nat. Biotechnol. **19,** 1141–1147

Bulte J. W., Duncan I. D., Frank J. A. (2002): *In vivo* magnetic resonance tracking of magnetically labeled cells after transplantation. J. Cereb. Blood Flow. Metab. **22,** 899–907

Deng C. X., Wynshaw-Boris A., Shen M. M., Daugherty C., Ornitz D. M., Leder P. (1994): Murine FGFR-1 is required for early postimplantation growth and axial organization. Genes Dev. **8,** 3045–3057

Doetschman T. C., Eistetter H., Katz M., Schmidt W., Kemler R. (1985): The *in vitro* development of blastocyst-derived embryonic stem cell lines: formation of visceral yolk sac, blood islands and myocardium. J. Embryol. Exp. Morphol. **87,** 27–45

Desbaillets I., Ziegler U., Groscurth P., Gassmann M. (2000): Embryoid bodies: an *in vitro* model of mouse embryogenesis. Exp. Physiol. **85,** 645–651

Ešner M., Pacherník J., Hampl A., Dvořák P. (2002): Targeted disruption of fibroblast growth factor receptor-1 blocks maturation of visceral endoderm and cavitation in embryoid bodies. Int. J. Dev. Biol. **46,** 817–825

Frank J. A., Miller B. R., Arbab A. S., Zywicke H. A., Jordan E. K., Lewis B. K., Bryant L. H. Jr., Bulte J. W. (2003): Clinically applicable labeling of mammalian and stem cells by combining superparamagnetic iron oxides and transfection agents. Radiology **228,** 480-487

Hahn P. F., Stark D. D., Lewis J. M., Saini S., Elizondo G., Weissleder R., Fretz C. J., Ferrucci J. T. (1990): First clinical trial of a new superparamagnetic iron oxide for use as an oral gastrointestinal contrast agent in MR imaging. Radiology **175,** 695–700

Hamm B., Staks T., Taupitz M., Maibauer R., Speidel A., Huppertz A., Frenzel T., Lawaczeck R., Wolf K. J., Lange L. (1994): Contrast-enhanced MR imaging of liver and spleen: first experience in humans with a new superparamagnetic iron oxide. J. Magn. Reson. Imaging **4,** 659–668

Hauger O., Frost E. E., van Heeswijk R., Deminière C., Xue R., Delmas Y., Combe C., Moonen C. T., Grenier N., Bulte

J. W. (2006): MR evaluation of the glomerular homing of magnetically labeled mesenchymal stem cells in a rat model of nephropathy. Radiology **238,** 200–210

He G., Zhang H., Wei H., Wang Y., Zhang X., Tang Y., Wei Y., Hu S. (2007): *In vivo* imaging of bone marrow mesenchymal stem cells transplanted into myocardium using magnetic resonance imaging: a novel method to trace the transplanted cells. Int. J. Cardiol. **114,** 4–10

Horák D., Babič M., Jendelová P., Herynek V., Trchová M., Pientka Z., Pollert E., Hájek M., Syková E. (2007): D-mannose-modified iron oxide nanoparticles for stem cell labeling. Bioconjug. Chem. **18,** 635–644

Jendelová P., Herynek V., DeCroos J., Glogarová K., Andersson B., Hájek M., Syková E. (2003): Imaging the fate of implanted bone marrow stromal cells labeled with superparamagnetic nanoparticles. Magn. Reson. Med. **50,** 767–776

Jendelová P., Herynek V., Urzdiková L., Glogarová K., Kroupová J., Andersson B., Bryja V., Burian M., Hájek M., Syková E. (2004): Magnetic resonance tracking of transplanted bone marrow and embryonic stem cells labeled by iron oxide nanoparticles in rat brain and spinal cord. J. Neurosci. Res. **76,** 232–243

Kostura L., Kraitchman D. L., Mackay A. M., Pittenger M. F., Bulte J. W. (2004): Feridex labeling of mesenchymal stem cells inhibits chondrogenesis but not adipogenesis or osteogenesis. NMR Biomed. **17,** 513–517

Keller G.M. (1995): *In vitro* differentiation of embryonic stem cells. Curr. Opin. Cell Biol. **7**, 862–869

Kroupová J., Horák D., Pacherník J., Dvořák P., Šlouf M. (2006): Functional polymer hydrogels for embryonic stem cell support. J. Biomed. Mater. Res. Part B, Appl. Biomater. **76,** 315–325

Martin G. R., Wiley L. M., Damjanov I. (1977): The development of cystic embryoid bodies *in vitro* from clonal teratocarcinoma stem cells. Dev. Biol. **61,** 230–244

Pacherník J., Ešner M., Bryja V., Dvořák P., Hampl A. (2002): Neural differentiation of mouse embryonic stem cells grown in monolayer. Reprod. Nutr. Dev. **42,** 317–326

Pacherník J., Bryja V., Ešner M., Hampl A., Dvořák P. (2005): Retinoic acid-induced neural differentiation of P19 embryonal carcinoma cells is potentiated by leukemia inhibitory factor. Physiol. Res. **54,** 257–262

Pera M. F., Reubinoff B., Trounson A. (2000): Human embryonic stem cells. J. Cell Sci. **113,** 5–10

Reimer P., Rummeny E. J., Daldrup H. E., Balzer T., Tombach B., Berns T., Peters P. E. (1995): Clinical results with Resovist: a phase 2 clinical trial. Radiology **195,** 489–496

Reimer P., Tombach B. (1998): Hepatic MRI with SPIO: detection and characterization of focal liver lesions. Eur. Radiol. **8,** 1198–1204

Robertson E. J. (1987): Embryo-derived stem cell lines. In: Teratocarcinomas and Embryonic Stem Cells: A Practical Approach. pp. 71–112, IRL Press, Washington DC

Simonsen C. Z., Ostergaard L., Vestergaard-Poulsen P., Røhl L., Bjørnerud A., Gyldensted C. (1999): CBF and CBV measurements by USPIO bolus tracking: reproducibility and comparison with Gd-based values. J. Magn. Reson. Imaging **9,** 342–347

Sipe J. C., Filippi M., Martino G., Furlan R., Rocca M. A., Rovaris M., Bergami A., Zyroff J., Scotti G., Comi G. (1999): Method for intracellular magnetic labeling of human mononuclear cells using approved iron contrast agents. Magn. Reson. Imaging **17,** 1521–1523

Smith A. G., Hooper M. L. (1987): Buffalo rat liver cells produce a diffusible activity which inhibits the differentiation of murine embryonal carcinoma and embryonic stem cells. Dev. Biol. **121,** 1–9

Syková E., Jendelová P. (2007): Migration, fate and *in vivo* imaging of adult stem cells in the CNS. Cell Death. Differ. **14,** 1336–1342

Tallheden T., Nannmark U., Lorentzon M., Rakotonirainy O., Soussi B., Waagstein F., Jeppsson A., Sjögren-Jansson E., Lindahl A., Omerovic E. (2006): *In vivo* MR imaging of magnetically labeled human embryonic stem cells. Life Sci. **79,** 999–1006

Vogl T. J., Schwarz W., Blume S., Pietsch M., Shamsi K., Franz M., Lobeck H., Balzer T., del Tredici K., Neuhaus P., Felix R., Hammerstingl R. M. (2003): Preoperative evaluation of malignant liver tumors: comparison of unenhanced and SPIO (Resovist)-enhanced MR imaging with biphasic CTAP and intraoperative US. Eur. Radiol. **13,** 262-272

Wang Y. X., Hussain S. M., Krestin G. P. (2001): Superparamagnetic iron oxide contrast agents: physicochemical characteristics and applications in MR imaging. Eur. Radiol. **11,** 2319–2331

Final version accepted: July 4, 2008